Measurement of Higgs Mass and Cross Section at a Linear Collider

Hai-Jun Yang Keith Riles*
Department of Physics, University of Michigan, Ann Arbor, MI 48109-1120, USA
(Dated: August 14, 2002)

We have studied the potential accuracy with which the Higgs boson mass and production cross section can be measured in the process $e^+e^- \to Z^0H, Z^0 \to l^+l^-, H \to X$ at a Linear Collider (LC) operated at 350 GeV and 500 GeV center-of-mass energies with integrated luminosities of 500 fb^{-1}. Using a Monte Carlo interpolation fit method, we find the Higgs mass can be determined with an accuracy of about 90 MeV at $\sqrt{s} = 350$ GeV, degrading to about 300 MeV at $\sqrt{s} = 500$ GeV for Higgs masses between 120 and 160 GeV. The relative precision of cross section is measured to be $\Delta\sigma/\sigma \sim 3\%$ at $\sqrt{s} = 350$ GeV and $\sim 5.5\%$ at $\sqrt{s} = 500$ GeV over the same mass range.

I. INTRODUCTION

Precise determinations of Higgs boson mass and cross section are important goals in future high energy e^+e^- linear collider experiments [1, 2]. Precision electroweak data in the framework of the Standard Model predict the mass of the Higgs boson, allowing a crucial cross check of electroweak symmetry breaking models if and when the Higgs boson is discovered. In addition, measuring the production cross section accurately allows determination of absolute Higgs decay branching ratios. Here we explore the accuracy with which the Higgs mass and cross section can be determined at a linear collider operated at 350 GeV and 500 GeV center-of-mass energies(CME), considering Higgs masses between 120 and 160 GeV. For this study, we use the 2001 North American baseline detector designs (LD for "Large" and SD for "Silicon").

II. ANALYSIS

The Higgs mass can be simply determined assuming recoil in the process $e^+e^- \to Z^0H, Z^0 \to \ell^+\ell^-, H \to X$ $(\ell = e, \mu)$. The recoil mass is defined as:

$$M_H^{recoil} = \sqrt{s - 2\sqrt{s} \cdot E_{\ell^+\ell^-} + M^2_{\ell^+\ell^-}}$$

where s is the center-of-mass energy squared, $E_{\ell^+\ell^-}$ is the energy of the lepton pair from Z^0 decay, while $M_{\ell^+\ell^-}$ is the pair's invariant mass. The main backgrounds of this analysis are $e^+e^- \to Z^0Z^0$, W^+W^-, but other sources of contamination, including Bhabha events, dimuon and two photos events are also investigated.

Monte Carlo events in this analysis were generated by the Pandora(V2.2)-Pythia(V3.1) package [3, 4] which includes initial state radiation, beamstrahlung, beam energy spread(full width is 1%), hadron fragmentation and final state QCD/QED radiation. In addition, the electron beam is polarized to −80%. The Java Analysis Studio(JAS) [5] package was used to analyze fast and full detector simulation events, assuming the LD and SD baseline detectors [1, 6, 7].

These studies are performed for a Next Linear Collider operated at center-of-mass energies of 350 GeV and 500 GeV with integrated luminosities of $500 fb^{-1}$ each, assuming Higgs mass between 120 and 160 GeV. Events are selected using a cut-based approach, according to the following criteria [8]:

(1) A candidate lepton must have an energy greater than 10 GeV
(2) The polar angle of a lepton must satisfy $|cos\theta_e| < 0.9$
(3) There must be at least 2 lepton candidates in the event
(4) The invariant mass of the lepton pair must lie within 5 GeV of the Z^0 mass
(5) The polar angle of two-lepton system must lie in the barrel region, $|cos\theta_{e^+e^-}| < 0.6$
(6) The opening angle between the two leptons should satisfy $|cos\theta_{e^+ \leftrightarrow e^-}| > -0.7$

Cut (5) is used to suppress Z^0Z^0 background, while Cut (6) reject background from W^+W^-. The selection efficiency for signal is about 48-50% for 350 GeV center-of-mass energy listed in TABLE I. The signal efficiency

*Electronic address: yhj@umich.edu,kriles@umich.edu

is higher, 55-56%, at a 500 GeV machine, mainly because the higher Lorentz boost of the leptons from Z^0 decay leads to a smaller average opening angle. For full SD events, however, the selection efficiency degrades 6-8% because of low track reconstruction efficiency in SD forward region.

$\sqrt{s}$	m_{Higgs}	Eff. of fast MC		Eff. of full MC	
(GeV)	(GeV)	LD(%)	SD(%)	LD(%)	SD(%)
500	120	55.2	55.2	55.5	49.7
	140	55.4	55.4	55.9	49.6
	160	55.2	55.3	56.8	50.4
350	120	49.9	50.0	48.2	41.2
	140	48.2	48.2	48.6	40.8
	160	48.0	47.9	47.6	38.7

TABLE I: Selection efficiencies of $e^+e^- \to ZH \to \mu^+\mu^- X$ for two baseline detectors, assuming NLC is operated at 350 and 500 GeV center of mass energies with Higgs masses between 120 and 160 GeV.

Beam energy spread with full width 1%, included in new version of Pandora(V2.2), makes Z recoil mass distribution much wider than that from without beam energy spread. The comparison is shown in FIG. 1. Compared with NLC ones, the Higgs mass accuracies and resolutions are improved by a factor of ~ 1.5 by using TESLA beam setup at 500 GeV CME, which has smaller beam energy spread(0.11% for positron and 0.48% for electron). Comparison of Z recoil mass spectra are shown in FIG. 3.

For the full detector simulation MC, the recoil mass distributions are a little worse than that from fast MC, shown in FIG. 2. Here, we use default beam setup(NLC500H) for $\sqrt{s} = 500$ GeV. Large discrepancy between recoil mass distributions of fast and full MC is seen for silicon detector. It's not surprising because the track reconstruction efficiency is quite low in SD forward region which eventually results in low selection efficiency.

Realistic detector simulations have been made with two baseline detectors, LD and SD for the process $e^+e^- \to Z^0H \to \mu^+\mu^- X$. FIG. 4 shows the Z recoil mass distribution for $\sqrt{s} = 500$ GeV and Higgs masses at 120(left plots) and 160(right plots) GeV. Backgrounds from WW and ZZ are smoothed to decrease the statistical fluctuation caused by small data samples. Red curves in the plots show fitted results by using gaussian and polynomial function. The similar Z recoil mass spectra for $\sqrt{s} = 350$ GeV are shown in FIG. 5

III. GAUSSIAN AND POLYNOMIAL FIT

Two mass-fit methods were explored for this study. In the first, the recoil mass spectra are fitted by the sum of analytic signal and background functions, with the signal described by a Gaussian distribution and the background by a polynomial, shown in FIG. 4 for $\sqrt{s} = 500$ and in FIG. 5 for $\sqrt{s} = 350$. A binned χ^2 fit is performed with two free parameters, the mass and the width. The Z recoil mass resolution is about 2.5-3.5 GeV at $\sqrt{s} = 350$ GeV and 5-8 GeV at $\sqrt{s} = 500$ GeV for the two baseline detectors, with better resolution seen for the SD detector, as shown in FIG. 6. Apparently, the recoil mass resolutions from full MC seems worse than that from fast MC. There is quite strong dependence of recoil mass resolution on low Higgs mass at $\sqrt{s} = 500$ mainly because the recoil mass peak of signal is diminished by large magnitude of background for low recoil mass, say, less than 130 GeV.

This analytic fitting technique yields a measured mass slightly larger than the true Higgs mass used in signal generation because of initial state radiation and beamstrahlung. This bias can be evaluated and corrected by fitting both data and Monte Carlo events with the same technique. The accuracy of such a mass determination is found to be about 110-160 MeV at $\sqrt{s} = 350$ GeV, degrading to 600-1200 MeV at $\sqrt{s} = 500$ GeV shown in FIG. 7. There is a large dependence upon low Higgs mass value for $\sqrt{s} = 500$ GeV, with lower masses yielding larger uncertainties because of higher background contamination.

What's more, we also study the dependence of Higgs mass accuracies and resolutions on integrated luminosities between 50 and 1000 fb^{-1}, corresponding plots shown in FIG. 10 and FIG. 11.

IV. MONTE CARLO INTERPOLATION FIT

The second fitting method used here is more accurate and is based on Monte Carlo interpolation. Several Monte Carlo samples are generated for different Higgs mass values surrounding a nominal desired central value and used to create fitting function shapes. For example, to estimate the measurement accuracy for a 140 GeV Higgs, we produced five Monte Carlo samples with M_{Higgs} = 138-142 GeV at 1 GeV spacing. Another Monte Carlo sample, generated at 140 GeV, is treated as "data" and its recoil mass distribution fitted to an interpolation of the Monte Carlo distributions, where again the goodness of fit is defined by a binned χ^2. The fitted parameters are the mass and the cross section. This method automatically corrects for biases due to any effects correctly modelled in the Monte Carlo simulation, and avoids degraded precision from non-optimal analytic modelling of resolution.

The Higgs mass accuracy obtained from the Monte Carlo interpolation fit is plotted vs the Higgs boson mass in FIG. 8. Here, results from the large detector and the silicon detector at $\sqrt{s}$ = 350 and 500 GeV are compared. The accuracy of Higgs mass measured with the LD detector design is about 90 MeV at $\sqrt{s}$ = 350 GeV, degrading to about 300 MeV at $\sqrt{s}$ = 500 GeV. Somewhat better accuracy is provided by the SD design. What's more, the dependence of Higgs mass accuracies on the integrated luminosities ranging from 50-1000 fb^{-1} are shown in FIG. 12.

The cross sections of $e^+e^- \to Z^0H \to l^+l^-X$ measured for the Higgs mass between 120 and 160 GeV are shown in FIG. 9. The relative precision of the cross section measurement is determined to be $\Delta\sigma/\sigma \sim 3\%$ at $\sqrt{s}$ = 350 GeV and $\sim$ 5.5% at $\sqrt{s}$ = 500 GeV for both baseline detector designs with nominal integrated luminosity 500 fb^{-1}. Furthermore, the relative errors of Higgsstrahlung signal cross section as a function of integrated luminosity are show in FIG. 13.

It is clear that for a light or intermediate Higgs mass, better precision on both mass and production cross section are obtained at $\sqrt{s}$ = 350 GeV than at $\sqrt{s}$ = 500 GeV. Better precision of higgs properties might be achieved by decreasing width of beam energy spread. Our results appear to be consistent with an earlier European study at 350 GeV which assumed a detector design with significantly worse momentum resolution [9].

We explore the dependence of Higgs mass measurement and cross section precision on charged particle tracking resolution elsewhere in Snowmass 2001 and Santa Cruz Retreat talks [8, 10]. Future studies will include incorporation of measured jets from hadronic Higgs decay with a kinematic fit.

Acknowledgments

We wish to thank Michael E. Peskin, Masako Iwasaki, Gary Bower, Tony Johnson, Mike Ronan, Wolfgang Wolkwowiak, Bruce A. Schumm, Rick van Kooten, John Jaros and Norman Graf, for kind help and many constructive discussions. This work is supported by the National Science Foundation of the United States under grant PHY-9984997.

[1] T. Abe et al. (American Linear Collider Working Group) (2001), resource book for Snowmass 2001, Colorado.
[2] J. A. Aguilar-Saavedra et al. (ECFA/DESY LC Physics Working Group) (2001), hep-ph/0106315.
[3] M. E. Peskin (1999), see also, http://www-sldnt.slac.stanford.edu/nld/new/Docs/Generators/PANDORA.htm, hep-ph/9910519.
[4] T. Sjostrand, Comp. Phys Comm. **82**, 74 (1994).
[5] T. Johnson, Proceedings of the Inter. Conf. on Comp. in High Energy Physics **(CHEP 98)** (1998), SLAC-PUB-7963.
[6] B. Schumm (2001), snowmass 2001 proceedings.
[7] L. C. Tracking-Group (2001), see http://www-mhp.physics.lsa.umich.edu/~keithr/LC/baselines_mar01.html.
[8] H. J. Yang and K. Riles (2001), snowmass 2001 proceedings.
[9] P. Garcia-Abia and W. Lohmann (1999), hep-ex/9908065.
[10] H. J. Yang and K. Riles (2002), at UC Santa Cruz Retreat talks.

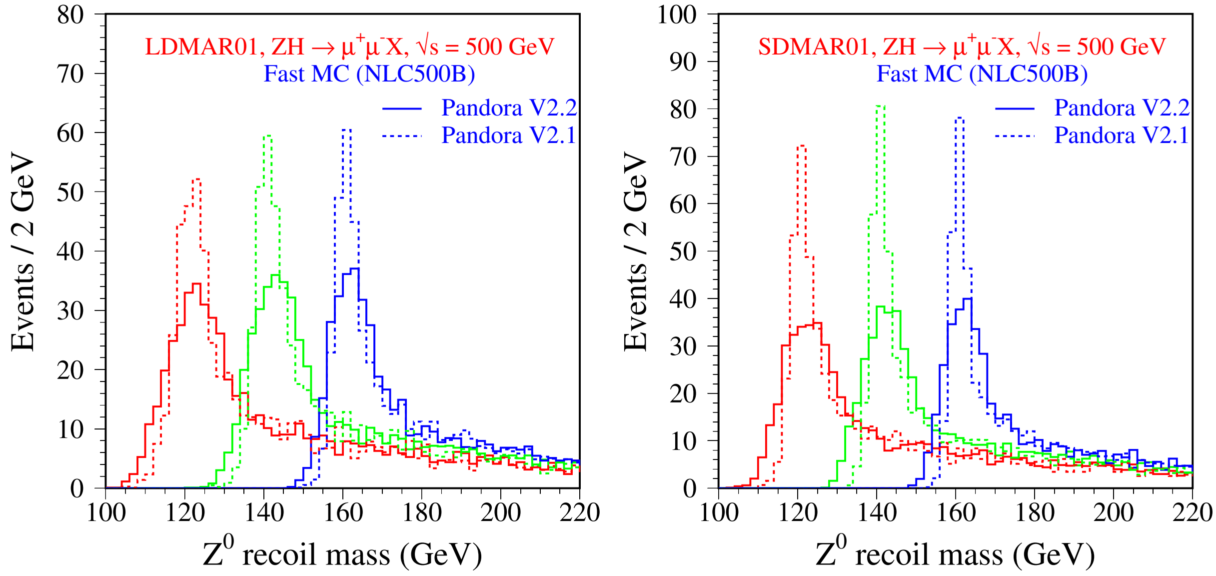

FIG. 1: Left – comparison of Z recoil mass distributions of $e^+e^- \to ZH \to \mu^+\mu^-X$ from fast MC for $\sqrt{s}=500$ GeV and Higgs masses at 120(red), 140(green) and 160(blue) GeV, which are produced by Pandora V2.2(solid lines) and V2.1(dotted lines) and simulated by large detector. Right – the corresponding recoil mass distributions for Silicon Detector.

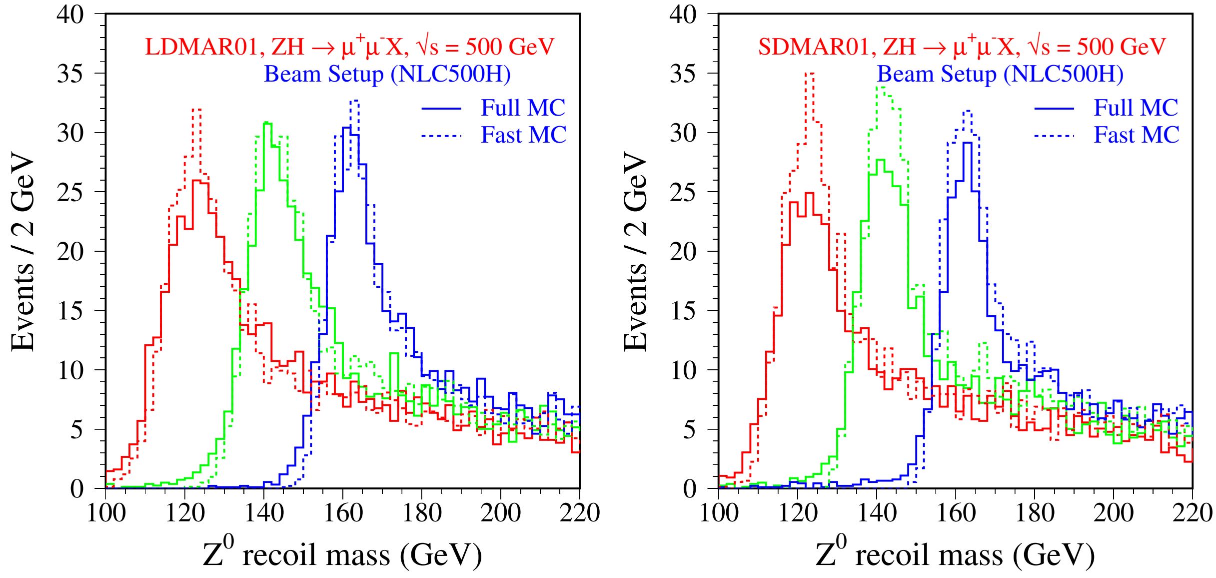

FIG. 2: Left – comparison of Z recoil mass distributions of $e^+e^- \to ZH \to \mu^+\mu^-X$ from Fast and Full MC for $\sqrt{s}=500$ GeV and Higgs masses at 120(red), 140(green) and 160(blue) GeV, which are produced by Pandora V2.2 and simulated by large detector. Right – the corresponding recoil mass distributions for Silicon Detector.

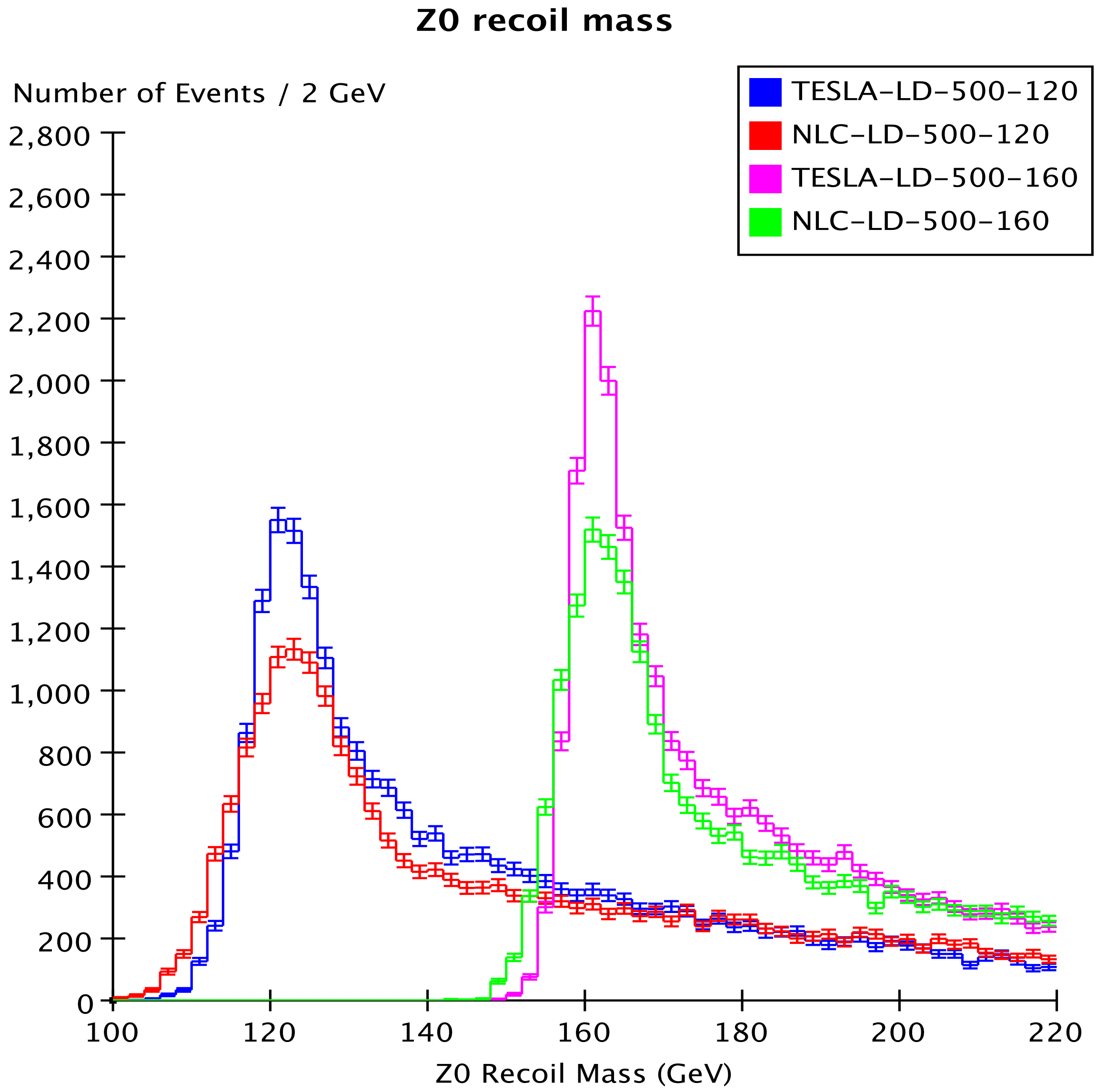

FIG. 3: Comparison of Z recoil mass spectra for NLC and TESLA at 500 GeV CME, with 120 and 160 GeV Higgs. Histograms in blue(120 GeV Higgs) and magenta (160 GeV Higgs) show Z recoil mass from fast MC sample with TESLA 500 beam setup. Histograms in red(120 GeV Higgs) and green(160 GeV Higgs) represent Z recoil mass spectra from fast MC sample with NLC 500 beam setup.

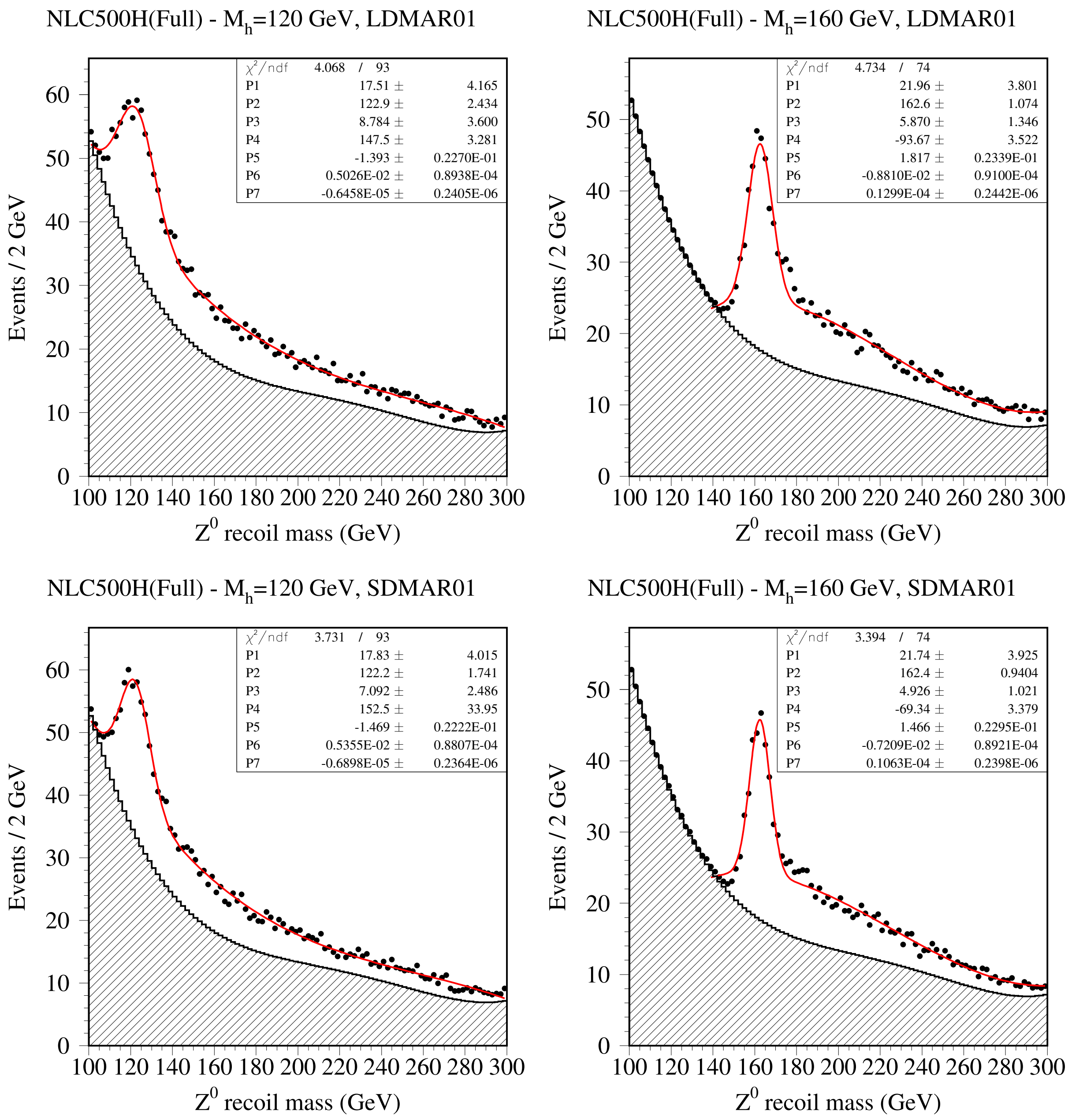

FIG. 4: The Z recoil mass spectra from full detector simulation. Top – the recoil mass distributions of $e^+e^- \to Z^0H \to \mu^+\mu^-X$ for LD with Higgs boson masses at 120(top left), 160(top right) GeV, along with the background contributions from Z^0Z^0 and W^+W^-(hatached area) at $\sqrt{s} = 500$ GeV. Red curves in the plots show fitted results by using gaussian and polynomial function. Bottom – the corresponding recoil mass distributions for the Silicon Detector.

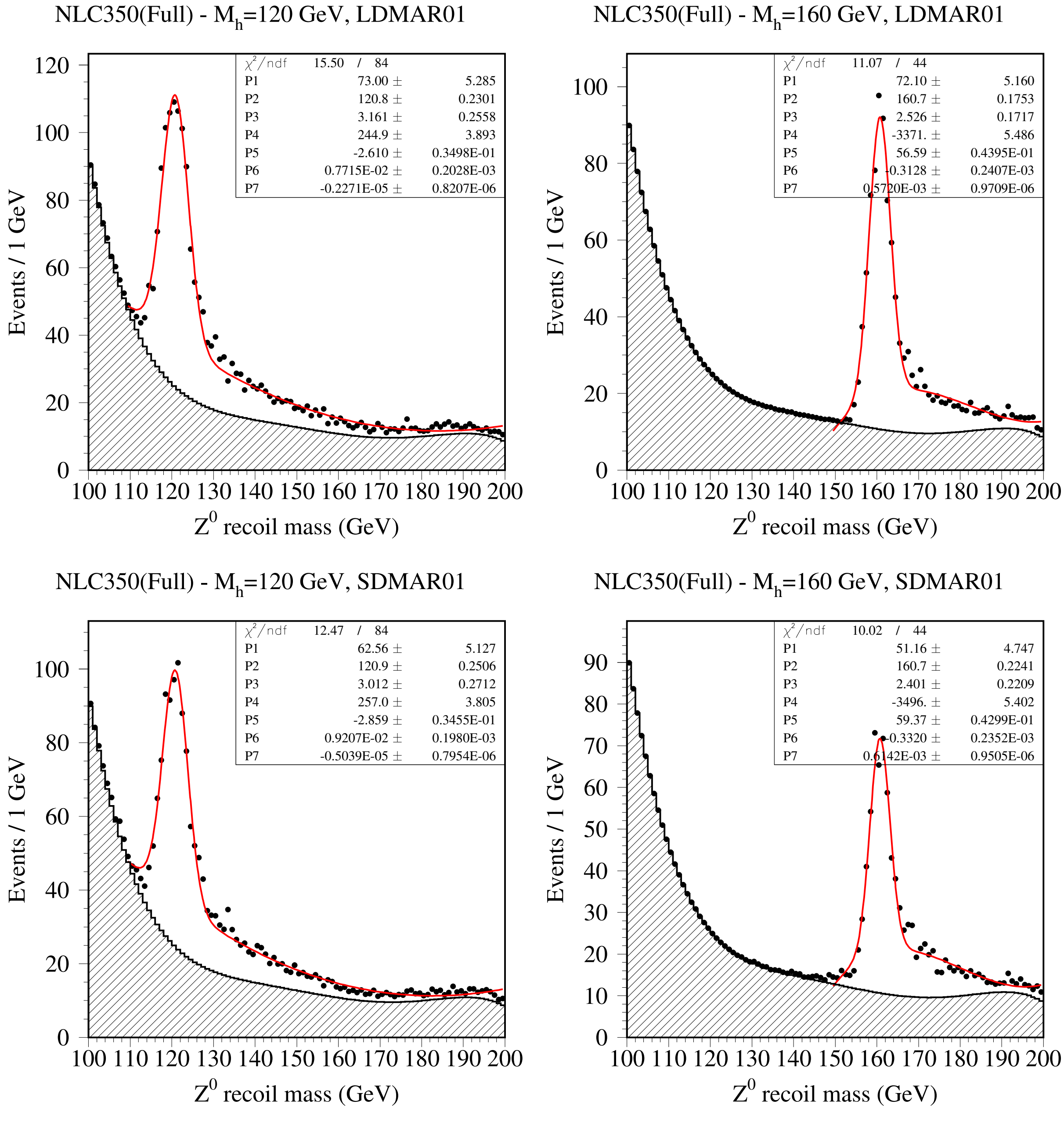

FIG. 5: The Z recoil mass spectra from full detector simulation. Top – the recoil mass distributions of $e^+e^- \to Z^0H \to \mu^+\mu^-X$ for LD with Higgs boson masses at 120(top left), 160(top right) GeV, along with the background contributions from Z^0Z^0 and W^+W^-(hatached area) at $\sqrt{s} = 350$ GeV. Red curves in the plots show fitted results by using gaussian and polynomial function. Bottom – the corresponding recoil mass distributions for the Silicon Detector.

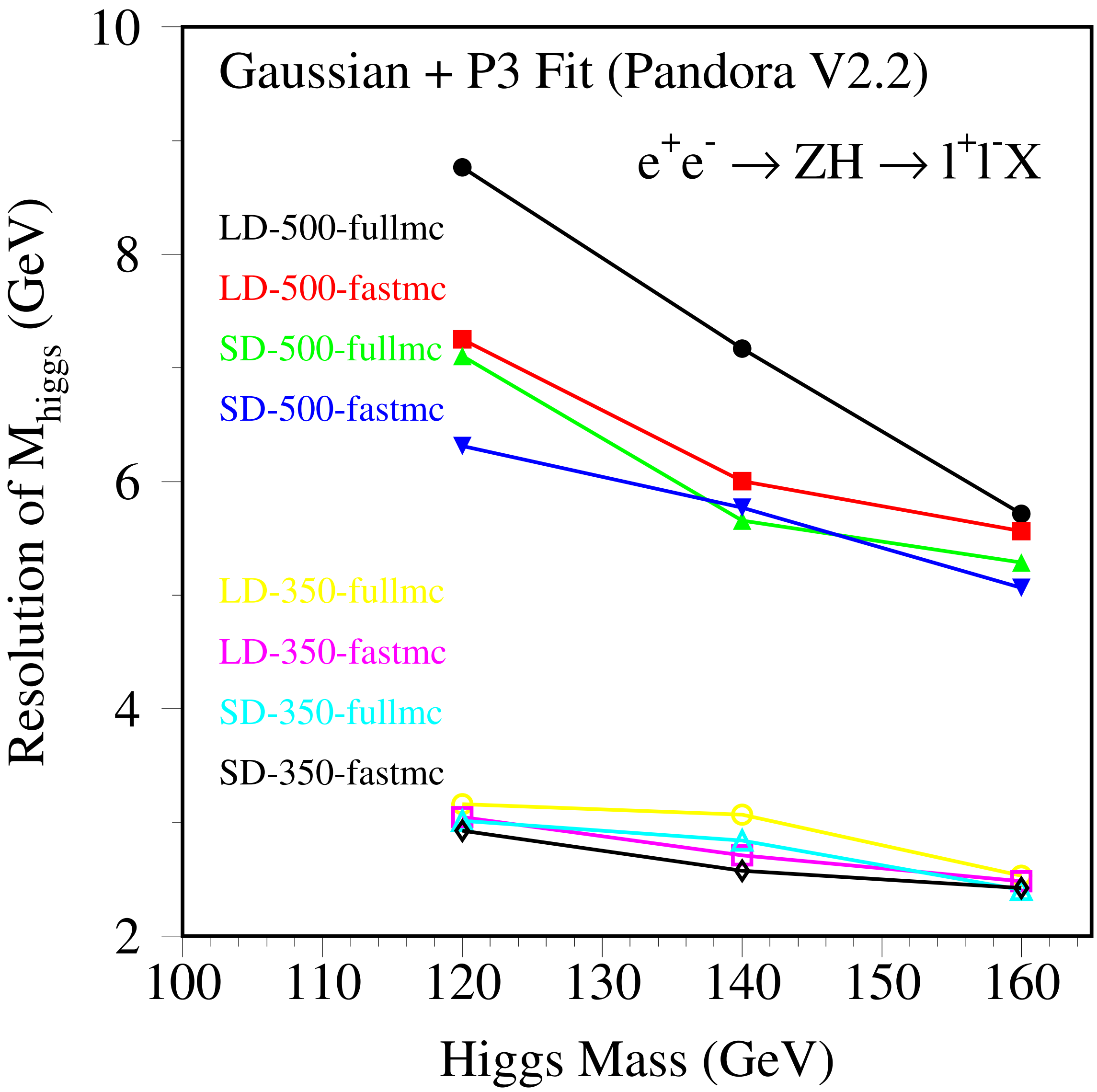

FIG. 6: The Z recoil mass resolution of $e^+e^- \to Z^0H \to l^+l^-X$ fitted by gaussian and polynomial function vs Higgs mass for fast and full MC at $\sqrt{s} = 350$ and 500 GeV with the LD and SD baseline designs.

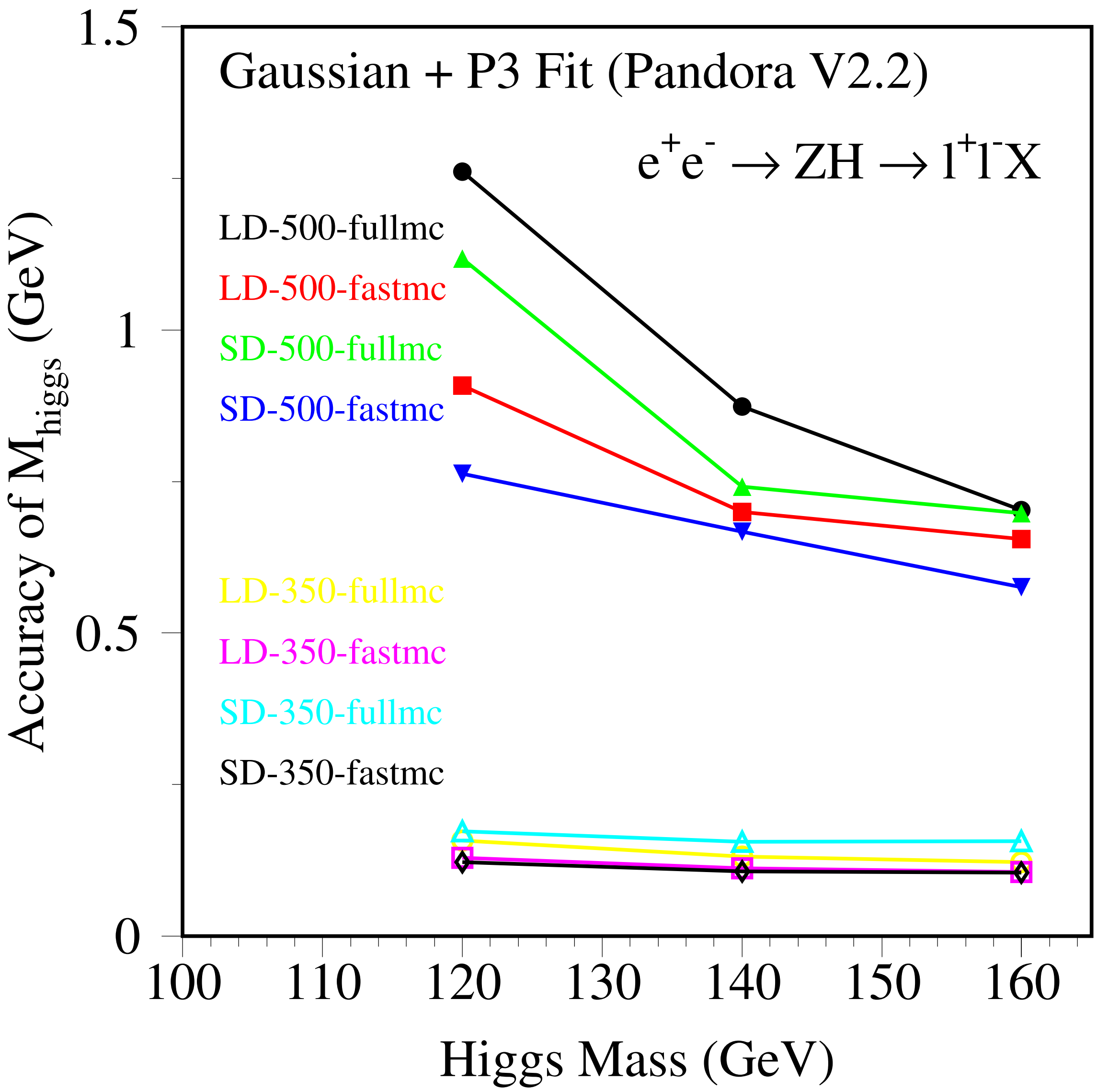

FIG. 7: The Higgs mass accuracy of $e^+e^- \to Z^0H \to l^+l^-X$ fitted by gaussian and polynomial function vs Higgs mass for fast and full MC at $\sqrt{s} = 350$ and 500 GeV with the LD and SD baseline designs.

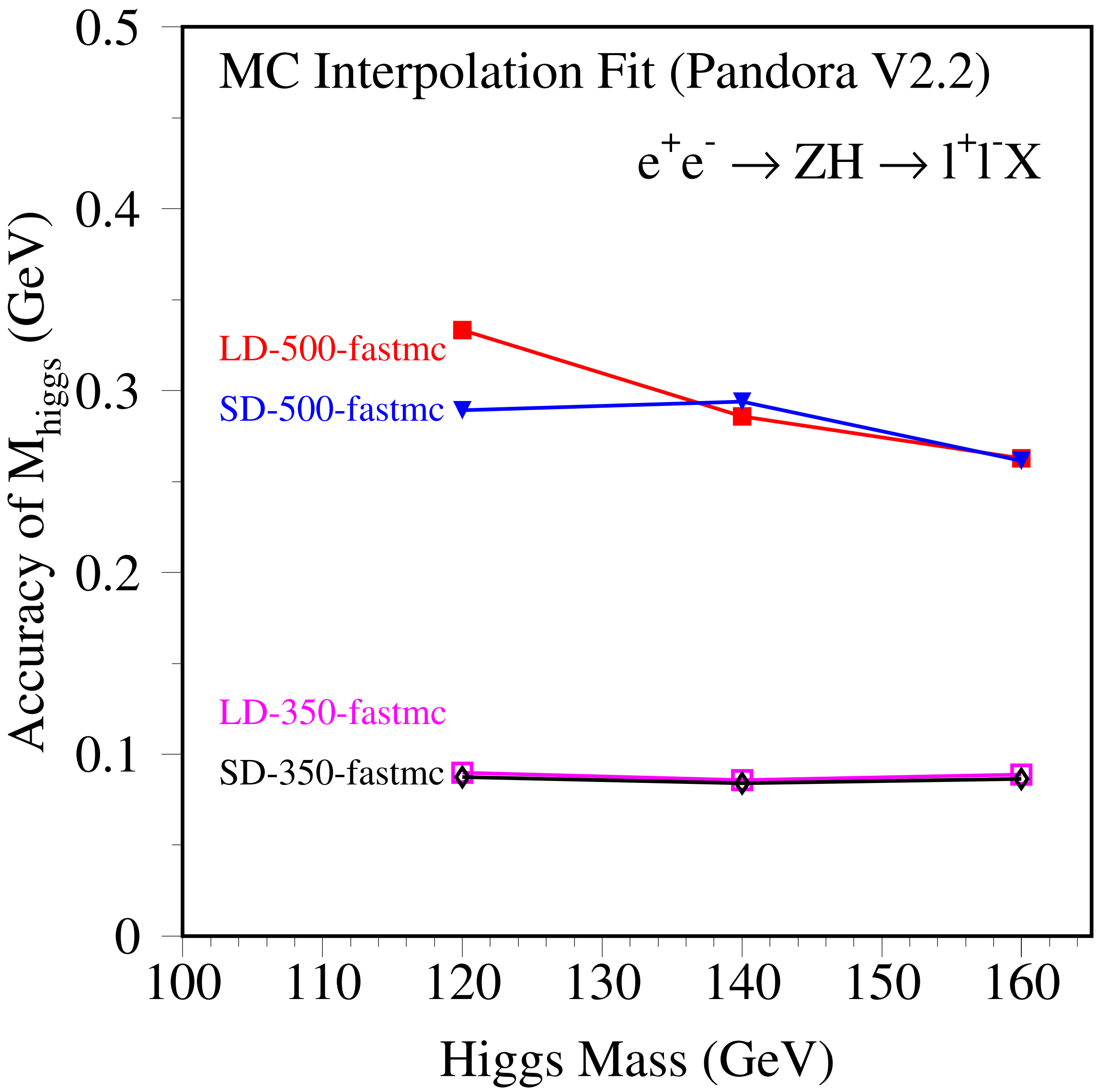

FIG. 8: The Higgs mass accuracy of $e^+e^- \to Z^0H \to l^+l^-X$ fitted by monte carlo interpolation technique vs Higgs mass for fast MC at $\sqrt{s} = 350$ and 500 GeV with the LD and SD baseline designs.

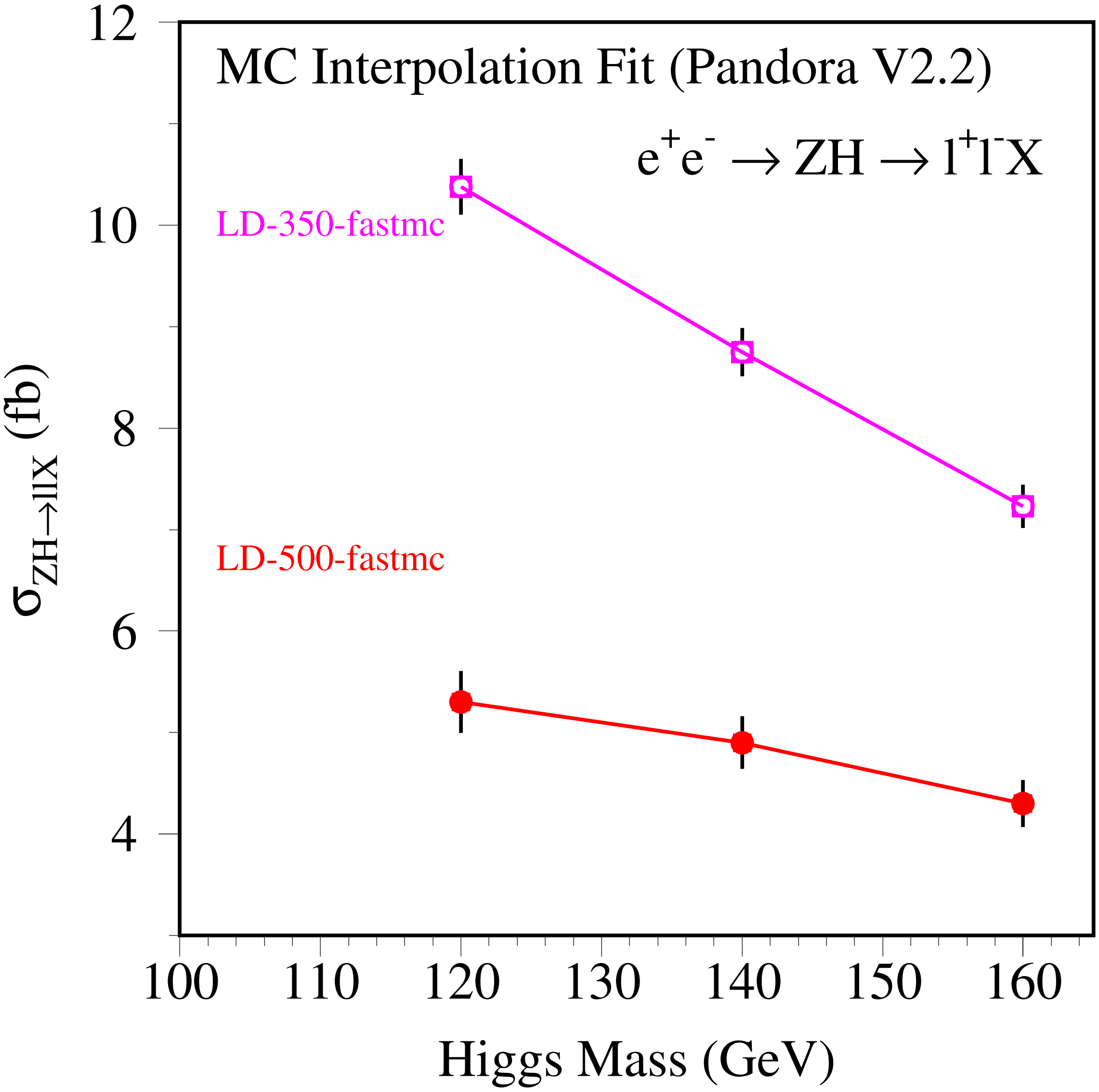

FIG. 9: The cross section of signal as a function of the Higgs boson mass, red points with error bars are the cross sections at $\sqrt{s}$ = 500 GeV, magenta points with error bars are the cross sections at $\sqrt{s}$ = 350 GeV, assuming an integrated luminosity of 500 fb^{-1}. The relative precision of the cross section measurement is determined to be $\Delta\sigma/\sigma \sim 3\%$ at $\sqrt{s}$ = 350 GeV and $\sim 5.5\%$ at 500 GeV for both baseline detector designs.

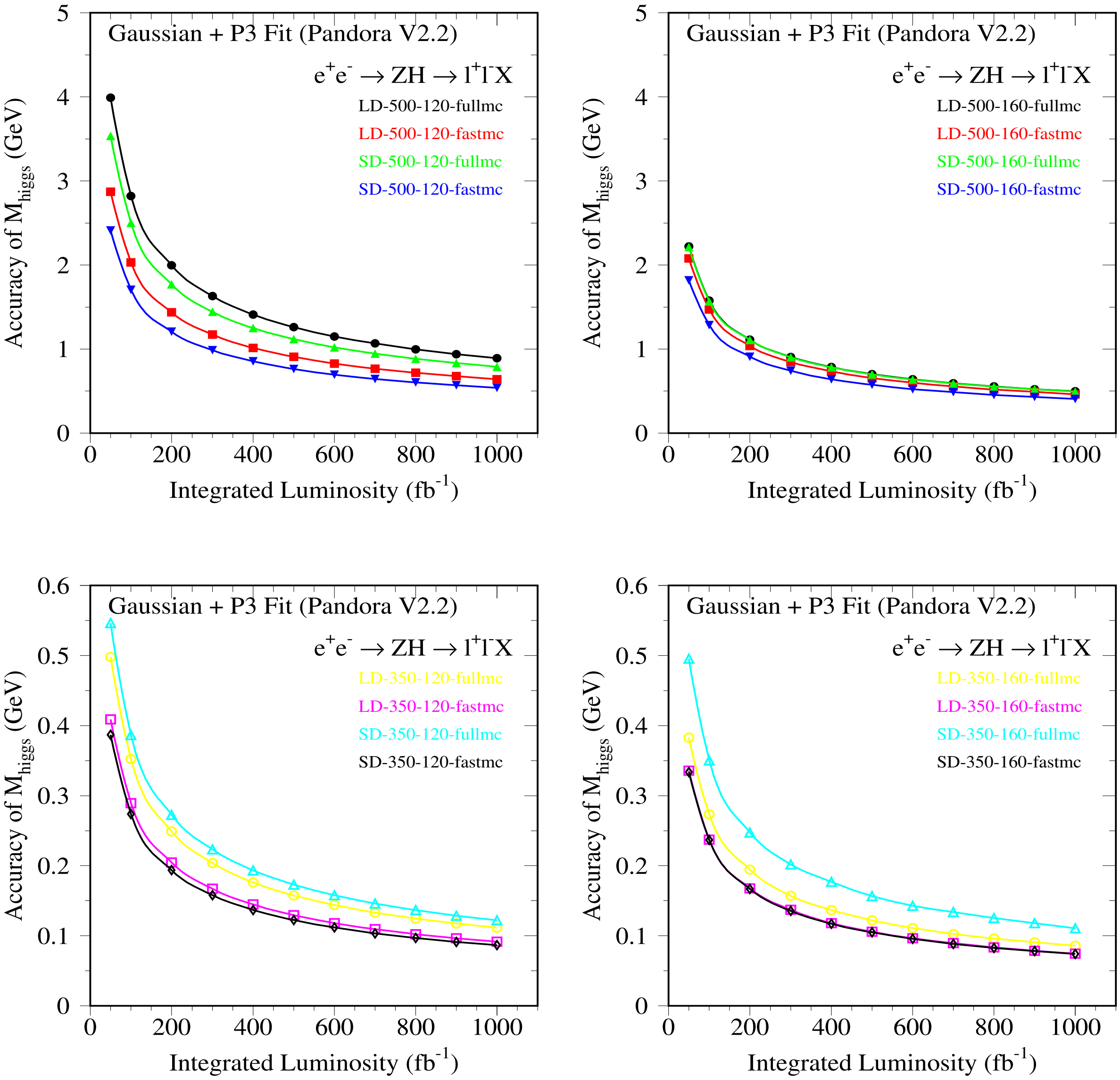

FIG. 10: Accuracy of Higgs mass vs integrated luminosity ranging from 50-1000 fb^{-1}. Here we use gaussian + polynomial(p3) function to fit signal and backgrounds. In top left plot, Points in black and green show accuracies of Higgs mass from full MC for LD and SD, respectively, with 120 GeV Higgs and 500 GeV CME. Better results are seen for the corresponding fast MC samples, shown in red and blue points. Top right plot shows similar results, only change Higgs mass assumption to 160 GeV. Better Higgs mass accuracy is derived because of lower background contamination. The bottom two plots show corresponding results from 350 GeV CME.

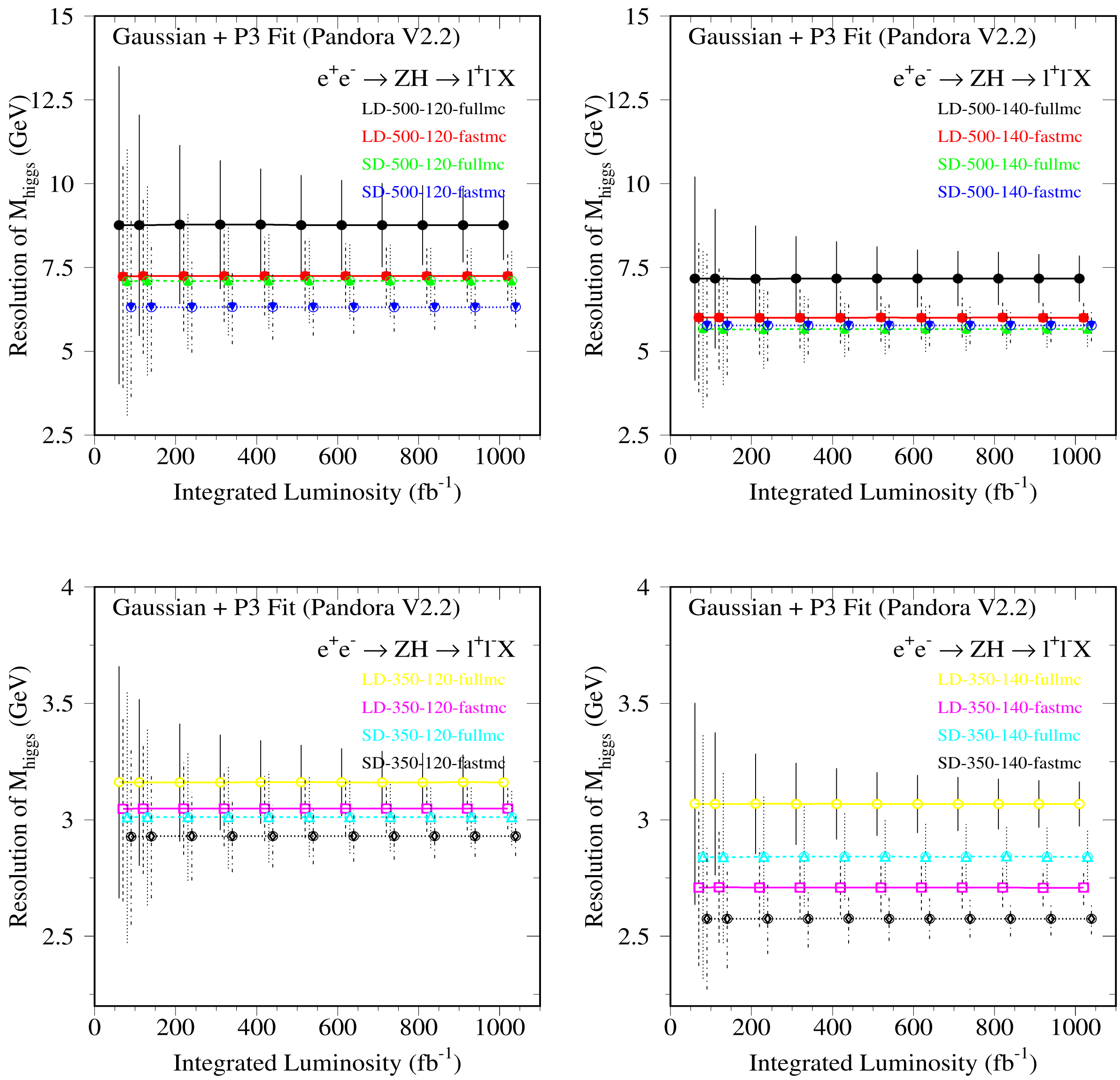

FIG. 11: Fitted resolution of Higgs mass as a function of integrated luminosity. Here, resolution is a measure of Higgs mass width. With the increasing of the integrated luminosity, the resolutions themselves won't change too much, but their uncertainties became smaller. The top two plots show Higgs mass resolutions from 500 GeV CME, The resolutions show moderate dependence on low Higgs mass, varies from 5 to 9 GeV, with higher Higgs mass yielding better resolution. Compared with 500 GeV CME, the Higgs mass resolutions can be improved by a factor 2 or more by operating NLC at low CME, 350 GeV, the results are shown in the bottom two plots.

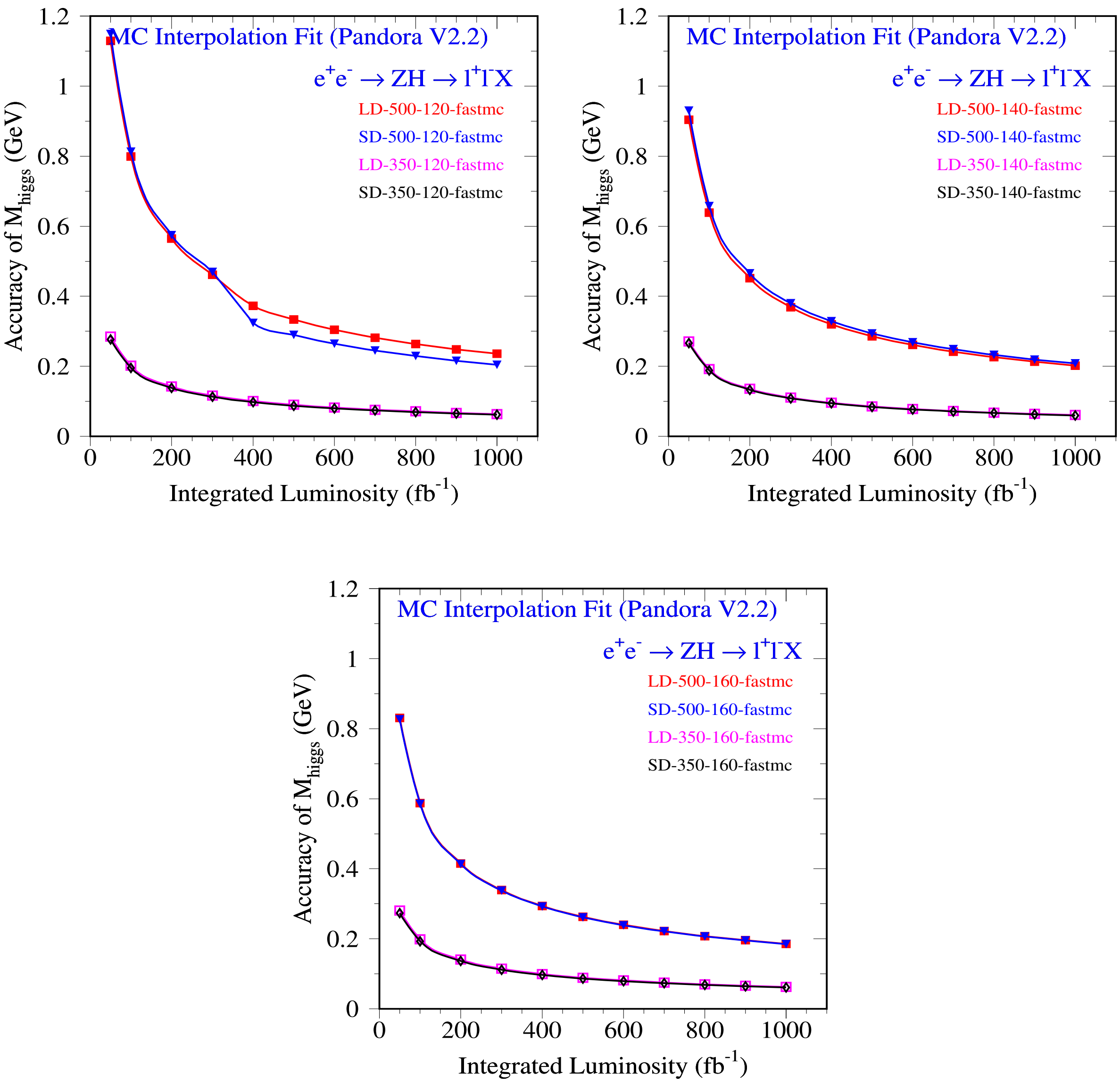

FIG. 12: Accuracy of Higgs mass measured by monte carlo interpolation technique as a function of integrated luminosity. Points in red and blue in top left plot show accuracies of Higgs mass from LD and SD, respectively. Here we assume 500 GeV CME and 120 GeV Higgs. Points in magenta and black represent results from 350 GeV CME. The top right and bottom center plots show accuracies of Higgs mass for 140 and 160 GeV Higgs, respectively. From these plots, comparable accuracy, about 200 MeV, are forseen for 100 fb^{-1} data at 350 GeV CME or 1000 fb^{-1} at 500 GeV CME.

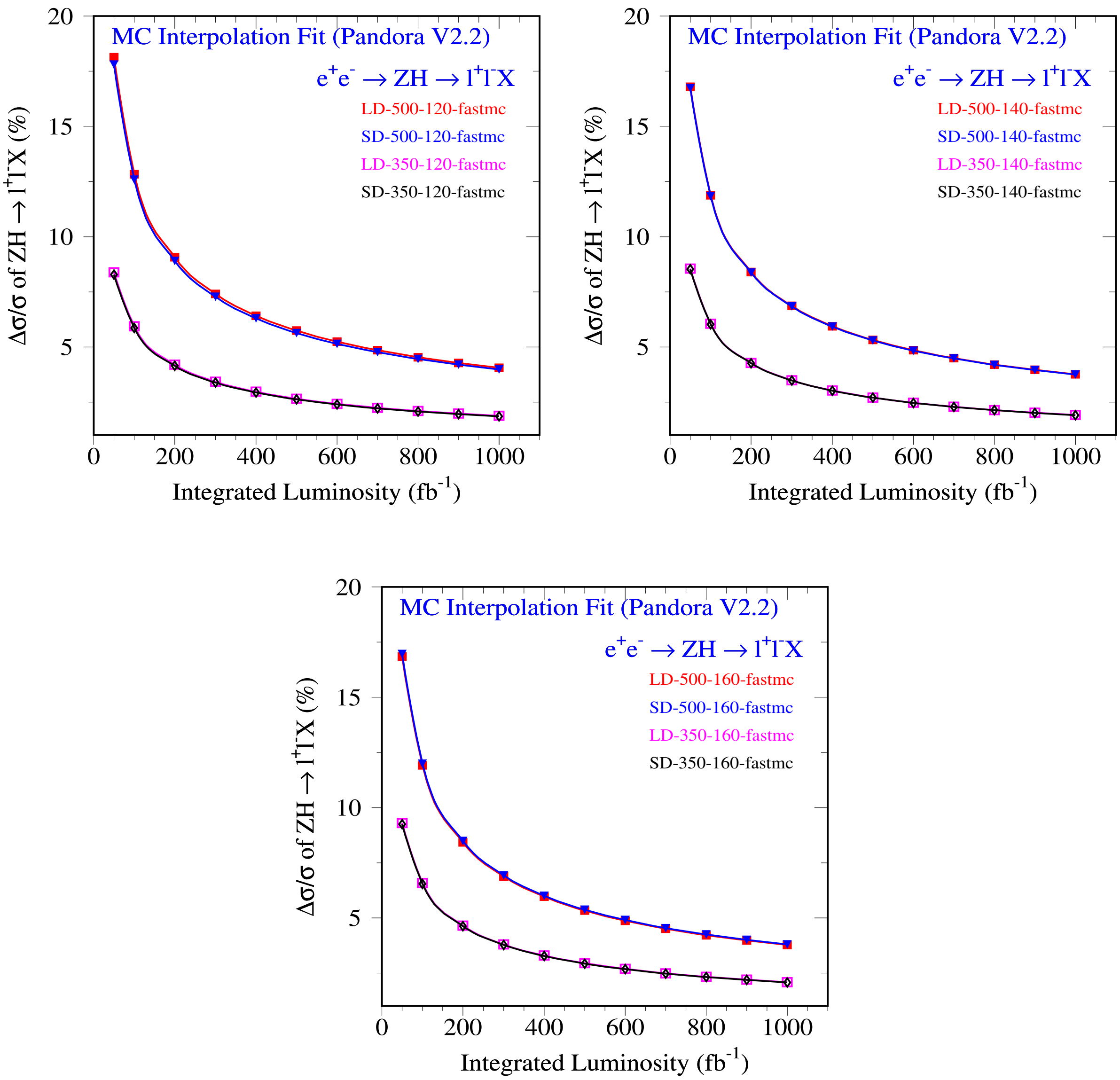

FIG. 13: These plots show relative errors of Higgsstrahlung cross section estimated by MC interpolation technique as a function of integrated luminosity for Higgs masses between 120 and 160 GeV. Curves in red and blue represent relative errors of cross section for 500 GeV CME, while curves in magenta and black show relative errors for 350 GeV CME. For nominal integrated luminosity, 500 fb^{-1}, the relative errors is 5.5% for 500 GeV CME, and 3% for 350 GeV CME.